

An IoT-based data analysis system: A case study on tomato cultivation under different irrigation regimes

Martina Galaverni ^a, Giulia Oddi ^{b,*}, Luca Preite ^c, Laura Belli ^b, Luca Davoli ^b, Ilaria Marchioni ^a, Margherita Rodolfi ^a, Federico Solari ^c, Deborah Beghè ^d, Tommaso Ganino ^{a,1}, Giuseppe Vignali ^{c,1}, Gianluigi Ferrari ^{b,1}

^a Crop and Plant Science (Cro.P.S.) Lab, Department of Food and Drug, University of Parma, Italy

^b Internet of Things (IoT) Lab, Department of Engineering and Architecture, University of Parma, Italy

^c Department of Systems Engineering and Industrial Technologies, University of Parma, Italy

^d Department of Economics and Management, University of Parma, Italy

ARTICLE INFO

Keywords:

Water stress
Internet of Things
Smart agriculture
Digital twin
Data collection

ABSTRACT

The exploitation of modern technologies in heterogeneous farming scenarios with different crops cultivation is nowadays an effective solution to implement the concept of Smart Agriculture (SA). Following this approach, in this study the tomato plants' response to different irrigation regimes is investigated through the implementation of an Internet of Things (IoT)-oriented SA data collection and monitoring system. In particular, the experimentation is conducted on tomatoes grown at three different irrigation regimes: namely, at 100%, 60%, and 30% of the Italian irrigation recommendation service, denoted as Irriframe. The proposed platform, denoted as *Agriware*, is able to: (i) evaluate information from heterogeneous data sources, (ii) calculate agronomic indicators (e.g., Growing Degree Days, GDD), and (iii) monitor *on-field* parameters (e.g., water consumption). Different plant-related parameters have been collected to assess the response to water stress (e.g., Soil Plant Analysis Development (SPAD), chlorophyll content, fluorescence, and others), along with leaf color and final production evaluations. The obtained results show that the best irrigation regime, in terms of plant health and productivity, corresponds to 60% of Irriframe, allowing significant water savings for the cultivation.

1. Introduction and related works

Nowadays, it is widely accepted that modern technologies and monitoring systems are expedient to improve productivity and quality in several contexts, including Smart Agriculture (SA). In fact, the application of precision agriculture techniques in heterogeneous farming scenarios, also in the presence of various types of plants, can act as an *enabler* for farmers interested in enhancing their cultivations. To this end, the Internet of Things (IoT) paradigm, referring to an approach in which cooperating heterogeneous technologies (including hardware, software, and networking components) enable real-world objects to collect data from the environment, is one of the most popular and interesting approaches to be applied to SA-oriented scenarios. In fact, the deployment of IoT sensors and actuators enables to collect information, in a wide sense, from the environment, the soil, and the overall farming conditions, thus facilitating crops' monitoring and

management, as well as enhancing agricultural efficiency and precision (Dagar et al., 2018). Moreover, the use of IoT technologies in SA-oriented scenarios is broad and versatile, with several studies focusing on data collection and monitoring across different types of crops. As an example, Kim et al. (2018) propose a framework collecting data through IoT devices to predict the presence of diseases and pests in *strawberry* plants; Falconit et al. (2020) detail a monitoring system that remotely controls and automates the condition of *eggplant* and *tomato* plants; Hnatiuc et al. (2022) propose an IoT-based architecture for monitoring a *vineyard* environment, in order to achieve autonomous data storage and processing.

Additionally, IoT technologies allow to improve both *quality* and *yield*, while reducing resources' waste (e.g., water and electricity consumption, costs, etc.). As an example, in Dong et al. (2024), the implementation of a low-cost sensor monitoring system, measuring soil moisture, improves the efficiency of irrigation water usage, saving 30% of water, yet maintaining the same marketable yields. Moreover,

* Corresponding author.

E-mail address: giulia.odd@unipr.it (G. Oddi).

¹ The authors contributed equally to the study.

the system presented in Lakshmi et al. (2023) allows to achieve 46% water usage reduction, through an IoT-based architecture, monitoring the irrigation schedule and employing a Long Short Term Memory-Recurrent Neural Network (LSTM-RNN) for a 1-day soil moisture level forecasting. Kanthavel et al. (2022) propose an algorithm targeting an effective utilization of resources and electricity in a dynamic agriculture environment, allowing a more efficient energy management. Another relevant aspect investigated in the state of the art refers to edge-fog-cloud architectures that can be adopted in SA scenarios, to reduce energy consumption, carbon dioxide (CO₂) emissions, and network traffic, and to improve the performance with respect to traditional cloud-based architectures (Alharbi and Aldossary, 2021). This technology *continuum* can automate tasks across different domains, such as irrigation, pest detection, and pesticide spraying, with minimal intervention from farmers (Jani and Chaubey, 2022).

Focusing on the communication technologies suitable to SA scenarios, where IoT devices are generally deployed in wide outdoor areas, the *Long Range Wide Area Network* (LoRaWAN) protocol (de Carvalho Silva et al., 2017), defined by the no-profit (LoRa Alliance, 2024), is well-known and commonly used for its effectiveness in long-range communication and its ability to operate efficiently, even in the presence of obstacles. In fact, the LoRaWAN protocol has a significant potential for IoT agricultural applications (e.g., soil, plants and air monitoring, irrigation, etc.), as discussed by Miles et al. (2020). To this end, if compared to other wireless IoT protocols – such as Zigbee (IEEE 802.15.4, defined by the Connectivity Standard Alliance, 2024) and WiFi (IEEE 802.11 g, defined by the WiFi Alliance, 2024) – LoRaWAN offers significant advantages in range and power efficiency (Sadowski and Spachos, 2020). As a further example, Zhang et al. (2022) present a LoRaWAN-based irrigation system providing a robust plant production control in an outdoor environment. Moreover, LoRaWAN might help in achieving precise soil moisture content's control, subsequently performing irrigation operations by using environmental parameters as input data (Seyar and Ahamed, 2023). Similarly, in Rohith et al. (2021) is described how sensors data (namely, moisture and temperature) can be exploited to automate the watering process.

The information collected by LoRaWAN-enabled IoT devices (as well as those based on alternative communication technologies) can enable the definition of digital models supporting the management of various processes. Despite this problem, the limited application of the Digital Twin (DT) paradigm in agriculture is highlighted in Preite et al. (2023b). In particular, this is due to modest investment opportunities for farmers, mis-information, and complex correlations between living and non-living structures. Purcell et al. (2023) state that DTs provide several advantages in different fields by digitally reproducing the behavior of complex systems, which represent the physical counterpart. Under this perspective, different configurations can be tested in order to optimize the physical domain and determine the safest and most effective solutions. As stated in Davoli et al. (2024), the application of DTs in agriculture is attractive for widespread agricultural cultivations with a clear industrial connection (such as tomato crops for canning industry).

Tomato (*Solanum lycopersicum* L.), counting an annual global production of around 186 million tonnes, is the most produced vegetable worldwide, as stated by FAO (2023). Tomato has widely adapted to most climatic regions of the world; however, stressful environmental conditions can decrease the crop's yield potential, as detailed in Gerszberg and Hnatuszko-Konka (2017). Moreover, climate change is greatly affecting water resources worldwide, especially in semi-arid areas, such as the Mediterranean countries where, despite the increased water scarcity, irrigation demands are projected to gradually increase to guarantee food security, as detailed in Cramer et al. (2018). Therefore, for vegetables such as tomato, whose water demand is almost totally met with irrigation, new water saving strategies need to be developed to overcome the gap between the supply and the demand of water, and to maintain highly satisfactory yields, as discussed in Cramer

et al. (2018) and Giuliani et al. (2017). Recently, different research studies demonstrate the feasibility of the application of reduced water stress levels on tomato plants without affecting crop yield and quality, as discussed in Giuliani et al. (2016, 2017), Patanè et al. (2011, 2020) and Valcárcel et al. (2020). In particular, Patanè et al. (2011) show that basing the irrigation on crop evapotranspiration (ET_c), defined by Jensen (1968) as “the rate of evapotranspiration for a given crop at a given stage of growth when water is not limiting and other factors such as insects, diseases, and nutrients have not materially restricted plant development”, allows to achieve a 48% water saving (without significant reductions in marketable yield) using a 50% ET_c restoration. Similarly, Giuliani et al. (2016) test different irrigation regimes and obtain the highest marketable yield with the regulated deficit irrigation set at 60 – 80 – 60% of the maximum ET_c. Finally, Obaideen et al. (2022) discuss on how smart irrigation systems, based on data acquisition (sensors), irrigation control, wireless communication, data processing and fault detection, have recently emerged as a new technique for the automation of irrigation and the optimization of water resources.

On the basis of the previous considerations, in this paper we present an innovative IoT-oriented platform for heterogeneous SA information collection and management, aiming at facilitating the monitoring of crop growth and crop health status. The proposed platform allows to collect and process heterogeneous IoT data to monitor crops' status and to save costs and water by forcing plants to a controlled water stress, without reducing, however, the final marketable yield. In fact, various automated irrigation systems have been found to be feasible and cost-effective tools for optimizing water resources for agricultural production (Gutiérrez et al., 2014; Boyaci et al., 2024).

The rest of the paper is organized as follows. In Section 2, a description of the materials and methods applied to the developed real testbed is provided. Section 3 presents several results obtained through plants' measurements and data analysis, while Section 4 discusses the obtained results. Finally, in Section 5 we draw our conclusions and outline future works.

2. Methods and materials

2.1. Experimental crop setup

Tomato plants (*Solanum lycopersicum* L. cv. HEINZ 1301) have been cultivated at the “Azienda Agraria Sperimentale Stuard (2024)”, located in Parma, Italy (60 m a.s.l., 44°48'29.888"N, 10°16'29.074"E). In particular, the HEINZ 1301 variety has been chosen as it is characterized by medium-early maturity, determinate growth habit, good vigor, and a great yield of round, slightly elongated fruits. The experimental activity has been carried out in a silty loam soil in which chemical and physical characteristics corresponded to the following conditions: organic matter: 19.6 g kg⁻¹; pH: 8.2; total N: 1.14 g kg⁻¹; assimilable P (P₂O₅): 26 mg kg⁻¹; exchangeable K: 0.3 meq kg⁻¹. More in detail, the monitored area is composed by three 90 m-long experimental rows and, as shown in Fig. 1, boundary rows are used to separate the experimental rows from each other, in order to prevent undesirable cross-interference between the different irrigation regimes.

Tomato plants were transplanted at the four-leaf stage, on June 1, 2023, with rows placed at 1.5 m distance from each other and with 0.23 m within plants. For each experimental row, three blocks consisting of 13 plants were set out and spaced between each other by 20 buffer plants. During the first three weeks after transplanting, 118.8, 90, and 180 units ha⁻¹ of N, P, K, respectively, were distributed. During the crop season, additional amounts of N, P, K were added for a final amount of 180, 90 and 200 ha⁻¹, respectively. Finally, experimentation and monitoring activities have been performed between June 29, 2023 and September 13, 2023, when tomatoes were harvested and analyzed.

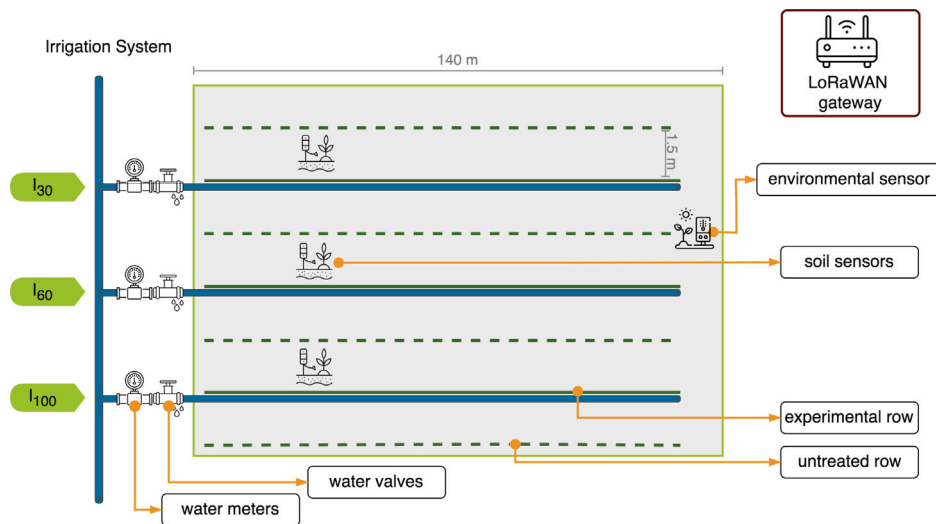


Fig. 1. Experimental setup of the tomato crop of the “Azienda Sperimentale Stuard” farm in Parma, Italy.

2.2. Water management

The irrigation system of the monitored crop has been controlled to associate a different watering regime with each experimental row. More in detail, the tomato irrigation has been scheduled according to the watering recommendations provided by the Italian (Irriframe, 2024) platform, a national cloud service developed by the Water Boards Italian Association (*Associazione Nazionale Consorzi di gestione e tutela del territorio e acque irrigue*, ANBI (2024)), aiming at ensuring an efficient water resources usage in the agricultural sector. In fact, Irriframe defines the amount of water to be supplied to the crops and the corresponding irrigation timing, leveraging an Artificial Intelligence (AI)-based algorithm taking into account the crop location and the continuum water balance between soil, plant, and atmosphere. Whenever possible, the algorithm takes into account the required environmental data provided by local weather stations, while the soil models has been divided into three layers – namely, *surface*, *root*, and *above-root* – in order to evaluate (i) the water runoff from each of them and (ii) the corresponding amount of water exchanged with the layer underneath. Therefore, each layer in the Irriframe platform has been considered as a tank with a given capacity. The associated inflow and outflow rates have been explored according to the continuity equation and empirical pedotransfer functions, as mentioned in Battilani and Ventura (1997): precipitations, irrigations, and water uptake from the groundwater for humidity gradient supply water to the root layer, while evapotranspiration, percolation, and runoff water are considered as outflow rates. Then, under optimal conditions, the evapotranspiration has been calculated by multiplying the reference value obtained from the FAO formula, reported in Pereira et al. (2015), by the crop specific coefficient k_c (adimensional), updated daily. When water stress is detected, the evapotranspiration rate decreases and its volume is calculated considering the measured conditions.

The irrigation strategy also takes into account the growth stage of the crop by using the Growing Degree Days (GDD), an agronomic indicator, defined in Derscheid and Lytle (1981), that quantifies the accumulation of heat units over time, particularly during the plant growing season, serving as a metric for the amount of energy available for plant growth and development. This indicator is then used in combination with the daily temperature and the soil moisture to estimate the root system development. Additional details on the GDD index are discussed in Section 3.4.

As mentioned in Section 2.1, the main objective of the experimental setup is to assess the effects of drought stress on tomato plants. For this reason, regular autonomous irrigation, characterized by a quantity of

water equal to 100%, 60%, and 30% of the recommendation provided by the Irriframe service, respectively, is applied to the three experimental rows, starting at the beginning of the blooming phase. For the sake of completeness, it should be highlighted that the irrigation regimes corresponding to the 60% and 30% of the Irriframe’s recommendation have been set in order to evaluate the effects of mild and severe water stress conditions, respectively, on plants’ physiology and yield, in accordance with previous studies in which similar irrigation regimes had already been tested (Giuliani et al., 2016, 2017; Patanè et al., 2011, 2020; Valcárcel et al., 2020). From the transplanting to the blossoming phases, a watering value equal to 100% has been adopted to irrigate all the experimental rows, in order to avoid plant stress in the early stages.

For the sake of clarity, in the rest of the paper the following notation is used:

- I_{100} denotes the experimental line/row irrigated using the same amount of water recommended by the Irriframe platform (100%): $3244.85 \text{ m}^3/\text{ha}$;
- I_{60} denotes the experimental line/row irrigated with a quantity of water equal to the 60% recommended by the Irriframe platform starting from the blossoming phase: $2402.08 \text{ m}^3/\text{ha}$;
- I_{30} denotes the experimental line/row irrigated with a quantity of water equal to the 30% recommended by the Irriframe platform starting from the blossoming phase: $1170 \text{ m}^3/\text{ha}$.

Considering the crop’s irrigation system, the watering network is based on a lightweight, non-self-compensating drip line with built-in flat drippers, positioned every 30 cm and delivering a nominal flow rate of 1 l/h . In detail, this solution has been selected in order to maintain the existing watering infrastructure already used in the “Azienda Stuard” for all their cultivations, thus minimizing the impact of the experimentation on the farm activities. Beside crop deployment, a digital model of the irrigation system has been developed in Preite et al. (2023a) in a 1-dimensional lumped parameter simulation software (namely, the *Flawnex*, 2024 environment) to estimate the water distribution along the network and, consequently, the specific water quantity delivered to each plant at any operational condition (namely, the different water regimes applied to different lines) with a high degree of accuracy.

2.3. Tomato fruit yields and plant measurements

The crop was hand harvested between September 12, 2023 and September 13, 2023, when ripe fruits rate reached about 95%. During the harvest, marketable (healthy, red, and ripe fruits) and non-marketable (green, rotten or Blossom End-Rot (BER)) fruits have been

weighed separately to estimate the fruit yields (dimension: [t ha⁻¹] Fresh Weight, FW). The procedure has been repeated for all the three experimental rows, together with each row tomato size (dimension: [g]) that has been computed as the average weight of 100 tomatoes randomly selected. Afterwards, the Irrigation Water Use Efficiency (IWUE, dimension: [kg m⁻³]) index has been determined as the ratio between marketable yield (dimension: [kg]) and the total amount of water applied by irrigation (dimension: [m³]), as suggested in Patanè et al. (2020). Similarly, the Water Use Efficiency (WUE, dimension: [kg m⁻³]) index has been computed as the marketable yield (dimension: [kg]) divided by the sum of precipitation and irrigation water amounts (dimension: [m³]), as indicated in Giuliani et al. (2016).

Physiological measurements have been performed throughout the experiment at three different sampling epochs with a frequency of approximately 15 days: (i) at the early fruit development (S₁), (ii) at fruit breaking (S₂), and (iii) at light-red ripeness degree (S₃), corresponding to 71–75, 81, and 88 tomato growth codes, respectively, according to the Biologische Bundesantalt, Bundessortenamt und Chemische Industrie (BBCH) scale, a system of uniform coding of phenological development stages of a plant defined by Bleiholder et al. (2001). Measurements were recorded between 10:00 and 15:00 on the third, full-expanded and sun-exposed leaf. The chlorophyll content (denoted as Soil Plant Analysis Development, (SPAD)) was estimated *in-situ* using a portable chlorophyll meter (namely, the Konica Minolta SPAD-502 model): 4 readings per leaf per plant have been averaged for each block. The color of the same fully-expanded leaves are assessed using the Minolta Chroma Meter CR-400 portable tristimulus colourimeter, and results are reported in the L*, a*, b* (International Commission on Illumination (CIE) and Technical Committee ISO/TC 274, 2019). Chlorophyll fluorescence measurements have been performed on one intact leaf per block using a Handy Plant Efficiency Analyzer (PEA) manufactured by Hansatech Instruments, after 30 min of dark adaptation. The instrument settings are as follows: pre-illumination: 0.1 s; illumination: 1 s; number of flashes: 1; intensity: 2500 μmol m⁻² s⁻¹. Finally, the fluorescence parameters under investigation are the following (as detailed by Tobiasz-Salach et al., 2019): area (Area) above the fluorescence curve between F₀ and F_m; photosynthetic performance (denoted as PI-ABS); efficiency of light absorption (denoted as RC/ABS); measurement of forward electron transport, indicated by (1-V_j)/V_j, where V_j is the relative variable fluorescence in the step J at 2 ms (Hammami et al., 2024).

At the harvest time, the tomato's branch length (one per plant for each block) has been determined measuring the longest one. Then, one plant per block has been eradicated and its hypogeal and epigeal parts dried at 105 °C until constant weight for Dry Matter (DW) measurements, while a fully expanded tomato leaf from each block has been collected at each sampling time, frozen in liquid nitrogen, and stored at -80 °C until the analysis time. The chlorophyll extraction and determination were carried out using the method reported by Rodolfi et al. (2021).

2.4. Statistical analyses

Plant physiology (SPAD, leaf color, fluorescence parameters, and pigments content), production (fruit yields, fruit size, IWUE and WUE), and growth (branch length and biomass) data have been analyzed for mean and standard error using the R language (v.4.3.2), defined by the R Core Team (2024). In detail, data's normal distribution and homogeneity of variance have been checked in accordance to Shapiro and Wilk (1965) and Bartlett (1937). Whenever there has been both the normality of data and the homoschedasticity, the Analysis of Variance (AoV, defined in Ross and Willson (2017)) using the aov function defined in Chambers et al. (1992) has been conducted. Then, a two-way Anova has also been employed to evaluate the effect of the interaction of time and irrigation on physiological data. Significant results in the analysis of variance have been followed by the Tukey's post-hoc test

Table 1
Detail on the IoT devices adopted in the experimental testbed in Parma, Italy.

IoT device	Number of devices	Measured parameters	Units of measurement
Milesight UG67 Gateway	1	–	–
Milesight EM500 CO ₂	1	Air moisture Air temperature CO ₂ level Barometric pressure	%RH °C ppm hPa
Milesight EM500 SMTC	3	Soil moisture Soil temperature Electrical conductivity	%RH °C μS/cm
Talkpool OY1310 water meter	3	Water usage	m ³
Mclimate T-valve	3	Water temperature	°C

(defined in Nanda et al., 2021) for the multiple comparison of groups at 5% significance levels using agricolae and mulcompView packages (defined in Mendiburu, 2010; Graves et al., 2023). Not-normally distributed data have been subjected to the Fligner Killeen test for the homogeneity of group variance (as defined in Conover et al., 1981) and, subsequently, have been analyzed through the Kruskal–Wallis and Dunn post-hoc tests in the rstatix package (defined in Kassambara et al., 2020). Finally, the Pearson's correlation (denoted as ρ) between physiological data of the same crop stage has been calculated using the corplot package (defined in Wei et al., 2021), while ggplot2, ggpubr, and ggcorrplot packages have been employed for data visualization, as detailed by Kassambara (2023a,b) and Wickham (2016).

2.5. Monitoring IoT system

Considering the IoT infrastructure enabling continuous data collection and plants' status monitoring, various sensing devices have been deployed in all the three experimental rows. More in detail, the IoT architecture consists of a set of LoRaWAN devices communicating with a LoRaWAN (Milesight UG67, 2024) outdoor gateway deployed in the farm's main building, in order to cover the whole area. All the deployed IoT devices act as LoRaWAN's Class A end nodes, have been registered on the open source TheThingsNetwork (TTN, 2024) platform, and have been configured to transmit their collected information every 10 min. In the following, the considered types of sensing devices are detailed.

- **Milesight EM500-CO₂ (2024)**: an *environmental sensor* designed to measure CO₂ concentrations in harsh environments and also to collect information on near-crop environmental parameters (namely, air humidity, temperature, and barometric pressure).
- **Milesight EM500-SMTC (2024)**: a *soil sensor* specifically designed to be installed under the ground, measuring soil moisture, soil temperature, and soil electrical conductivity. Considering the monitored plant, the sensors have been positioned, for each line, at a 20 cm depth.
- **Talkpool OY1310 (2024)**: a LoRaWAN *smart meter* device allowing water usage measurement in the various lines.
- **Mclimate T-valve (2024)**: a *smart valve* allowing to get information on the status (open/close) of valves installed on pipes in the crop irrigation systems.

The total number of devices installed in the “Azienda Stuard” testbed and the measured parameters are detailed in Table 1, while a summary of the position of each device in the experimental crop is shown in Fig. 1.

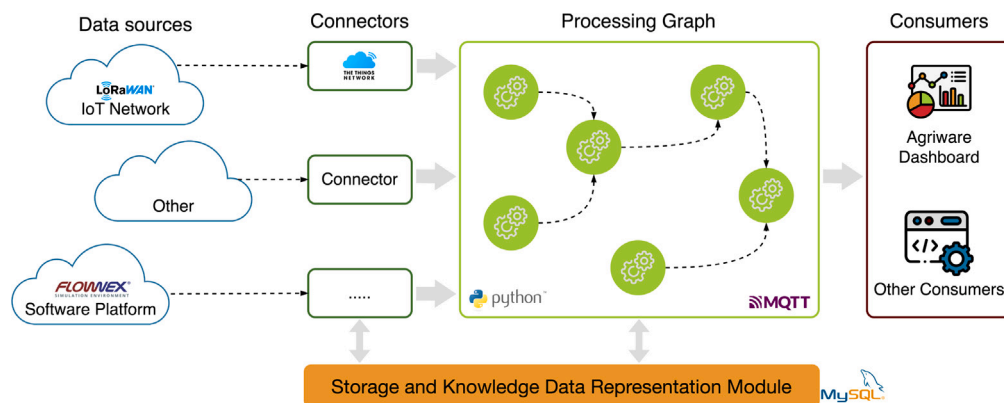


Fig. 2. Main components and their interaction of the proposed Agriware IoT-oriented SA platform.

2.6. Data acquisition platform

The information generated by the different IoT devices have been integrated in a general data acquisition platform, denoted as *Agriware*, specifically designed to manage and analyze, in a uniform way, the heterogeneous data sources in the field of SA applications, thus acting as a middleware, as detailed in Belli et al. (2023) and in Oddi et al. (2024). More in detail, the main objectives of the Agriware platform include: (i) the integration of information from heterogeneous data sources (mainly IoT device-generated data, but also manual plants measurements, information from other softwares, such as Flownex, etc.); (ii) the definition of processing modules from integrated data sources, in order to calculate indicators, as well as to get insights and to estimate data correlations of interest from an agronomic point of view; and (iii) monitoring of parameters (Table 1) related to a specific cultivation or crop, such as water consumption for irrigation. As a final step, data and information generated by the platform can be shared (e.g., through RESTful APIs) to external entities, generally denoted as *Consumers*. The different modules composing the overall Agriware architecture, their interactions, as well as the scope of each module, are shown in Fig. 2 and detailed in the following.

2.6.1. Data sources

The architecture of the Agriware platform has been designed to integrate and manage heterogeneous information from different origins. The first main category of data sources is represented by IoT devices, that can be easily integrated independently of their specific communication protocols (e.g., LoRaWAN, Wi-Fi, cellular 4G/5G, etc.) and data formats (e.g., JSON, CSV, XML, etc.). Besides that, also information generated by other software platforms are potential data sources for Agriware, independently of the specific integration mechanisms (e.g., REST APIs, WebSocket, etc.) and used data formats. In general, data sources can thus be seen as input stream for the overall platform.

2.6.2. Connectors

Connectors correspond to software modules allowing the integration of data streams from various sources. In particular, connectors mainly target (i) the integration into the platform of data of interest from data sources, such as IoT sensors or external platforms, and (ii) the interaction with other software modules in the architecture. Connectors are implemented for each class of data sources to be integrated in Agriware: in particular, in the instance deployed for the tomato experimentation, a TTN connector has been developed in order to acquire and parse data streams generated by the involved IoT devices. Moreover, a Flownex connector allows the integration of data related to the irrigation system digital model. Connectors have been developed as reusable and modular components using the Python language.

2.6.3. Processing graph

The Processing Graph module represents the Agriware core and allows general and configurable processing of data collected and integrated by previous components. More in detail, this module is structured with a layered architecture, where building modules are denoted as *Processing Units*, or *Layers*. Processing Units are custom software modules that can be uploaded in the Agriware platform, to perform specific processing tasks on one or more information streams. They allow to manage and manipulate the collected data generating new data streams that can also be input of other processing units, creating a completely configurable layered architecture for the Processing Graph module.

The routing of information generated in this module is managed through the Message Queuing Telemetry Transport (MQTT, 2024) protocol and organized in different topics (namely, each stream of data is associated with a unique MQTT topic). In the context of the described testbed, specific Processing Units have been developed, with the Python language, to calculate the following agronomic indicators, on the basis of IoT devices information: (i) GDD, (ii) Heat Units (defined in Machado et al., 2004), (iii) the Normal Heat Hours (NHH) curve (defined in Ferrante and Mariani, 2018) and (iv) statistical operations. It is noteworthy to highlight that the set of Processing Units can be easily extended if necessary, e.g., to execute complex operations and data fusion tasks, along with AI-based processing (e.g., for predicting sensor data). Indeed, Preite and Vignali (2024) reported an AI-based water supply management system able to achieve water and energy savings of up to 27% and 57%, respectively. In this application, Machine Learning (ML) algorithms and a Multi-Layer Perceptron (MLP) Artificial Neural Network (ANN) were trained with the data provided by the IoT network described in this paper.

2.6.4. Storage and knowledge data representation module

The Storage and Knowledge Data Representation Module of the proposed architecture is designed with the purpose of managing data normalization and storage. In particular, the first objective of this module is to perform data parsing and translation tasks to support a normalized and uniform data representation across the system. This is done in compliance with a specifically defined cross-layer SA taxonomy for the data integrated into the Agriware platform. The second objective is to maintain a set of relational databases, most of them based on MySQL, to store the historical information from Data Sources and Processing Units. This module allows the creation of a dataset – exploited in this paper and publicly available at Belli et al. (2024) – containing information on the tomato growing season and allowing continuous data monitoring and analysis. As a consequence, the presence of a persistent storage module simplifies the management of heterogeneous data sources: namely the information integrated by Connectors, as well as the information generated by the Processing Graph module.

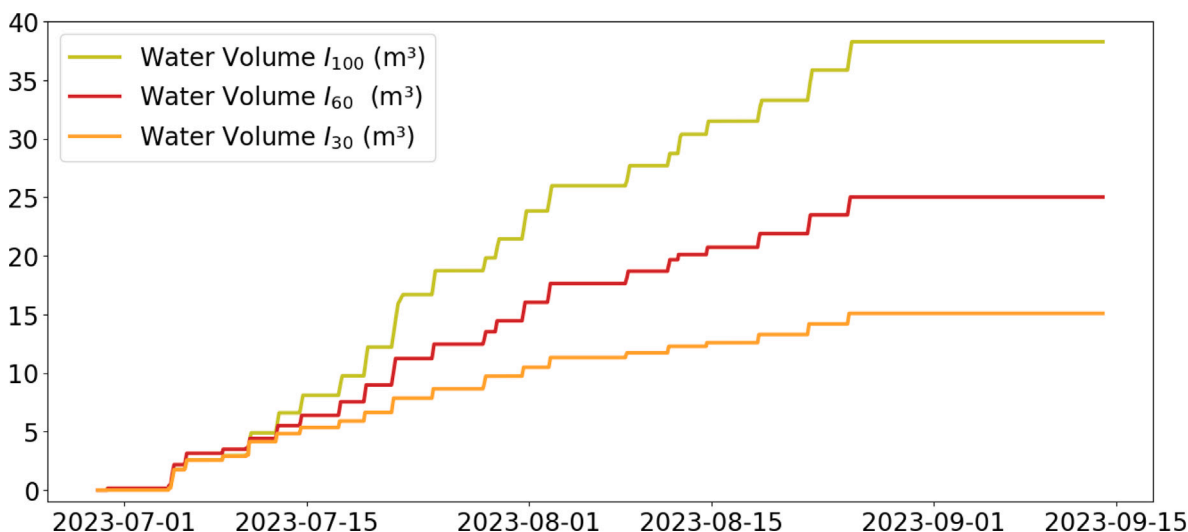


Fig. 3. Water volume irrigated in the experimental crop in the different irrigation regimes (I_{100} , I_{60} , I_{30}).

2.6.5. Consumers

The information integrated by Connectors and generated by Processing Units can be shared by the platform to other entities through APIs. These entities, generally denoted as *Consumers*, are external software modules with an interest in the generated data streams. In the context of the experimentation, the main Consumer entity is the Agriware web dashboard, specifically developed to share access and all the data related to the experimentation.

3. Results

As detailed in Section 2, the IoT network deployed in the experimental cultivation to monitor and control the experimental crop allows to determine the water consumption throughout the farming season. Fig. 3 shows the recorded water consumption of the three experimental lines during the entire observation period.

3.1. Fruit yield and irrigation water use efficiency

In the proposed experimental deployment, the effect of water stress on tomato yield has been investigated considering both marketable and non-marketable fruit fractions, with the latter including green and rotten production. As it is clearly reported in Table 2 and Fig. 4, I_{60} and I_{30} —resulted in a significant decrease in total production ($p = 0.01$) with a reduction of 28.58% and 49.22% for I_{60} and I_{30} , respectively. However, a strong impact ($p = 0.01$) on the average weight was observed only at I_{30} , where tomatoes were 29.09% lighter compared to those of the I_{100} . The marketable production responded to water stress similarly ($p = 0.003$).

Within the non-marketable fraction, significant differences due to irrigation were observed in the BER and green yields. Reduced water amounts significantly increased the production of tomatoes with BER ($p = 0.005$), representing 1.94% of the total yield for the I_{100} , 6.29% for the I_{60} , and 15.83% for the I_{30} . On the other hand, the green fruits yield was 4.3 times higher in I_{100} compared to I_{60} ($p = 0.009$), while no differences were seen in the rotten production. The three water regimes resulted in comparable ratios of marketable yield, but under I_{30} and I_{60} , a water saving of 19.47 m³ and 11.12 m³ were achieved (as detailed in Table 3). Finally, no differences were found in the irrigation use efficiency for the Marketable Yield IWUE (MYIWUE) and Total Yield IWUE (TYIWUE), regardless of the precipitations which were more efficiently exploited by I_{60} and I_{100} .

3.2. Plant measurements

In this work, the growth of tomato plants in response to irrigation has been also investigated. The obtained results show that under water stress conditions there was a greater, though not significant, development of the epigeal biomass representing the 83.53%, 79.80%, and 76.57% of the total dry weight for I_{30} , I_{60} and I_{100} , respectively. On the contrary, the length of tomato branches was significantly affected ($p = 10^{-4}$) by water stress, with branches for I_{60} and I_{30} being 8.31% and 21.45% shorter than those of the I_{100} (see Appendix for additional details).

3.3. Physiological measurements on tomato leaves

The SPAD values changed throughout the experiment due to time and irrigation. In fact, the results from a one-way ANOVA revealed that water stress affected positively the SPAD values in the first two samplings ($p = 8.04 \cdot 10^{-5}$ and $p = 9.4 \cdot 10^{-12}$) since the index for I_{30} and I_{60} irrigation was significantly higher compared to the control. By the end of the experiment, all three water regimes showed a decline of SPAD values, particularly in the case of I_{30} with a loss equal to 20.40% compared to the initial value (see Appendix for additional details). As shown in Fig. 5A, under water restrictions, an increase of chlorophyll type a (denoted as Chl a) content between the first and second sampling occurred, up to 37.03% for I_{60} which was then followed by a general decrease. Chlorophyll type b (denoted as Chl b) content changed throughout the season in a similar way, as displayed in Fig. 5B. The total chlorophyll (denoted as Chl tot) contents in the first half of the experiments for all the water regimes were comparable ($p > 0.05$), but the effect of water stress became significant ($p = 0.03$) at the third sampling epoch, when the difference under I_{100} and I_{30} irrigation was equal to 34.41% (as shown in Fig. 5C). The carotenoid content in tomato leaves under different water regimes was comparable at any time ($p > 0.05$) but, even if they all underwent a reduction throughout the experiment, the one-way ANOVA showed significant decrease throughout the trial only under water stress conditions ($p = 0.002$ for I_{60} , $p = 0.01$ for I_{30} irrigation), as shown in Fig. 5D.

The photosynthetic apparatus of tomato plants was monitored by studying the chlorophyll fluorescence via PI, RC/ABS, Area and (1-Vj)/Vj parameters, whose results are shown in Table 4. Results from a two-way ANOVA to evaluate the effect of time and irrigation revealed that time was responsible for the decline of the index ($p = 4.77 \cdot 10^{-8}$), with reductions up to 82.67% for I_{30} , while irrigation did not affect the photosynthetic performance at any sampling epoch. A declining trend

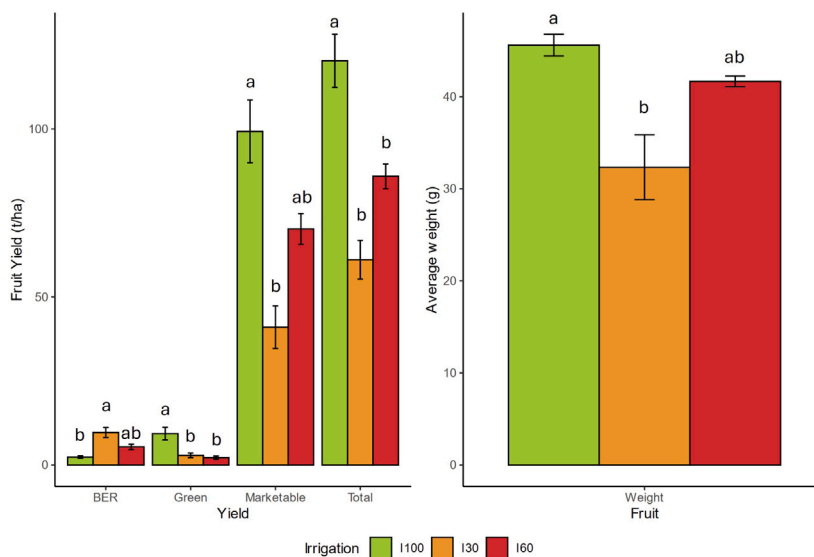


Fig. 4. Final tomato production obtained from the experimental deployment.

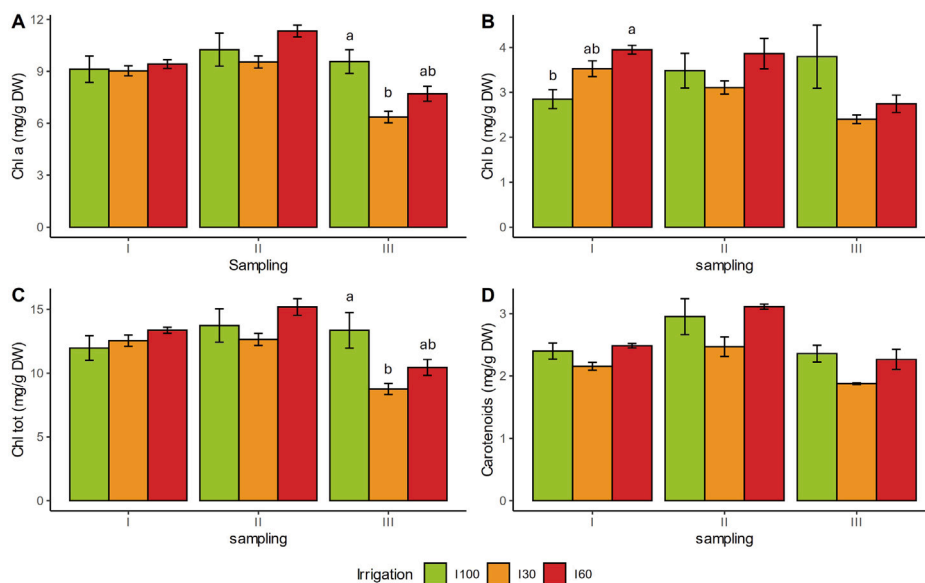


Fig. 5. Effect of water irrigation conditions on chlorophyll a (Chl a), chlorophyll b (Chl b), total chlorophyll (a + b) and carotenoids content during the water stress trial. Data presents the average \pm standard error. Different letters indicate significance at $p < 0.05$ by Tukey's test among the same sampling time. The absence of letters indicates not significant differences.

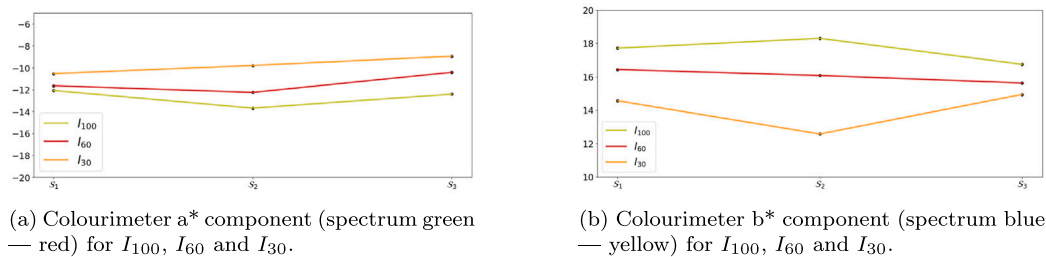


Fig. 6. Colourimeter a* and b* components for tomatoes' leaves during season (S₁, S₂, S₃).

Table 2Effects of irrigation treatments on total, marketable, green, and blossom-end rot fruit yield (t ha^{-1}) and fruit size (g) on processing tomato cv. Heinz 1301.

Treatment	Total yield	Marketable yield	Green fruit yield	BER fruit yield	Average weight
I_{30}	61.07 ± 9.96^b	41.00 ± 10.98^b	2.87 ± 1.20^b	9.67 ± 2.57^a	32.33 ± 3.53^b
I_{60}	73.48 ± 3.67^b	70.23 ± 4.57^{ab}	2.17 ± 0.47^b	5.40 ± 0.78^{ab}	41.67 ± 0.58^{ab}
I_{100}	120.27 ± 7.89^a	99.27 ± 9.35^a	9.33 ± 1.85^a	2.33 ± 0.37^b	45.60 ± 1.17^a

The data are reported in terms of mean \pm standard error. Different letters indicate statistically significant differences at $p < 0.05$ by Tukey's test.

Table 3

Effects of the irrigation treatments on the ratio of marketable yield, IWUE and WUE.

Treatment	Ratio of Marketable Yield (%)	Seasonal irrigation volumes (m^3)	TYIWUE (kg m^{-3})	MYIWUE (kg m^{-3})	TYWUE (kg m^{-3})	MYWUE (kg m^{-3})
I_{30}	66.50 ^a	23.36	34.50 ^a	23.16 ^a	19.08 ^b	12.81 ^b
I_{60}	81.81 ^a	31.71	35.76 ^a	29.24 ^a	22.42 ^{ab}	18.33 ^{ab}
I_{100}	82.28 ^a	42.83	37.06 ^a	30.59 ^a	25.73 ^a	21.23 ^a

The data are reported in mean. Different letters indicate significant differences at $p < 0.05$ by Tukey's test. TYWUE: total yield water use efficiency;

MYWUE: marketable yield water use efficiency.

Table 4Effects of the irrigation treatments on fluorescence parameters at S_1 , S_2 and S_3 .

Time	Water regime	PI	RC/ABS	Area	(1-Vj)/Vj
S_1	I_{30}	13.50 ± 1.57	2.86 ± 0.25	29.90 ± 2.40	0.76 ± 0.01
	I_{60}	10.88 ± 1.22	2.62 ± 0.17	29.92 ± 0.32	0.75 ± 0.01
	I_{100}	9.59 ± 0.77	2.40 ± 0.11	24.01 ± 1.58	0.74 ± 0.01
S_2	I_{30}	2.69 ± 1.22	1.38 ± 0.37	23.72 ± 3.88	0.54 ± 0.08
	I_{60}	3.37 ± 0.61	1.98 ± 0.52	28.79 ± 3.53	0.69 ± 0.05
	I_{100}	5.09 ± 1.35	1.74 ± 0.23	23.52 ± 0.93	0.66 ± 0.03
S_3	I_{30}	4.60 ± 0.29	1.00 ± 0.12	9.42 ± 0.84	0.58 ± 0.01
	I_{60}	4.52 ± 0.80	1.68 ± 0.13	17.91 ± 0.98	0.65 ± 0.02
	I_{100}	4.60 ± 1.19	1.65 ± 0.21	22.77 ± 1.13	0.65 ± 0.04

The data are reported in mean \pm standard error. Area must be multiplicatively $\cdot 10^3$ since it is expressed in thousands.

is also noted in RC/ABS parameter mainly due to time ($p = 8.86 \cdot 10^{-5}$) with losses up to 65.03% compared to the initial value under I_{30} . Similarly, the area and (1-Vj)/Vj values decreased because of time ($p = 1.5 \cdot 10^{-6}$ and $p = 0.001$). Besides, irrigation had a significant effect on the area at the last sampling epoch ($p = 2 \cdot 10^{-4}$). Similarly, the area and values (1-Vj)/Vj decayed over time ($p = 1.5 \cdot 10^{-6}$ and $p = 0.001$), but in the case of the area, there was also a significant impact of irrigation ($p = 0.02$).

The color of tomato leaves across the trial period was monitored measuring L^* , a^* , b^* values, which are reported in Table 12 (see Appendix for additional details) together with the SPAD values. In detail, a^* and b^* emerge as the most important Lab* color dimensions, serving as indicators of the levels of green and yellow hues, respectively. As illustrated in Fig. 6A, I_{30} displays elevated a^* values, indicating that the plants in this line exhibit less greenness. Moreover, the a^* component shows an increasing trend over time in both I_{100} and I_{60} . Consequently, providing 60% of the water requirement may be sufficient for the plants to grow properly. By the two-way ANOVA, results that the greenness of the leaves changed both for the effect of time ($p = 4.6 \cdot 10^{-12}$), irrigation ($p < 10^{-16}$) and their interaction ($p = 2 \cdot 10^{-5}$), showing differences from the very beginning of the trial.

Fig. 6B demonstrates that the b^* values of I_{30} show an increasing trend over time, while the b^* component of I_{100} decreases. This suggests a progressive yellowing of the leaves of the plants in line I_{30} . The b^* values of line I_{60} remain relatively stable throughout the entire season. These results imply that tomato plants in I_{30} tend to exhibit undesirable characteristics, such as apical rot and yellowing, under insufficient watering conditions, whereas irrigation with 60% of water need is sufficient for optimal plants growth. Similarly to the a^* values,

the leaves yellowness decreased during the experiment mainly because of the impact of water ($p = 2 \cdot 10^{-16}$) and the prolonged application of stress over time ($p = 0.01$).

To visually represent the colors of tomato plants, a conversion from the Lab* color scale to the RGB color scale was performed and the visual results are shown in Fig. 7. In particular, the color of the leaves in I_{100} remained relatively consistent throughout the entire season, as highlighted in Figs. 7(a), 7(d) and 7(g). The color of plants in I_{60} also remained consistent over time, with a slight yellowing in the final measurement, as shown in Figs. 7(b), 7(e) and 7(h). Instead, the RGB colors of the plants in I_{30} , illustrated in Figs. 7(c), 7(f) and 7(i), reveal a change in the color over time. In fact, towards the end of the summer, the plants in this line appeared more yellow compared to their status in June and to the other lines. Therefore, I_{30} proved to be the least effective, providing both the lowest percentage of sealable tomato production and wilted leaves with such a minimal water supply.

Correlations between the leaves' parameters at each sampling epoch are displayed in Fig. 11 (see Appendix for additional details). Some coefficients changed considerably during the experiment (e.g., SPAD - Chl a going from -0.2 at the first sampling epoch to 0.6 at the third one), while others (e.g., Area - Chl tot) were fairly stable (with correlation values ranging, over time, between 0.8 and 1).

3.4. IoT data analysis and processing

The Agriware platform described in Section 2.6, concentrating all IoT data streams related to the experimental crop, has allowed to carry out processing and analysis tasks. In detail, the data collected from the IoT devices have been analyzed to identify some correlations between them. Tables 5–7 present the Pearson's correlation values ρ of the parameters monitored by sensors in I_{100} , I_{60} and I_{30} , respectively.

Moreover, the implemented Processing Units in the Agriware middleware calculate various indicators, derived from data collected by sensors and of interest from an agronomic point of view. A dedicated Processing Unit has been developed to compute the GDD, which is based on the average daily air temperature (denoted as T_{avg}), measurable through environmental sensors, and the base temperature (denoted as T_{base}), also known as vegetation zero point, specific to the vegetative species under consideration, as highlighted by McMaster and Wilhelm (1997). The vegetation zero point represents the minimum biological temperature below which plants stop their vegetative activities. Another critical temperature for GDD calculation is the cutoff temperature (denoted as T_{cutoff}), representing the maximum temperature above which plants cannot grow. Once these values are known, the daily GDD

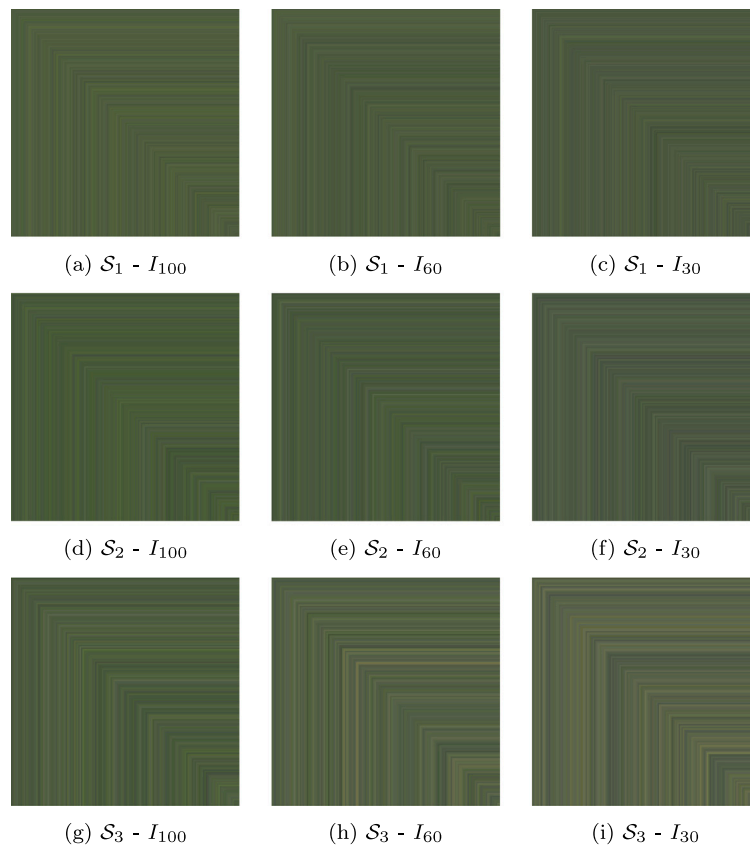


Fig. 7. Color of tomato leaves in RGB color scale during season (S_1 , S_2 , S_3).

Table 5

Pearson's correlations value of sensor's parameters tomato's line I_{100} .

Property	Electrical conductivity	Soil humidity	Soil temperature	CO ₂	Air pressure	Air temperature	Water volume
Electrical conductivity	1	0.835499	0.254875	-0.144756	-0.588404	0.427518	-0.724829
Soil humidity	0.835499	1	0.160898	-0.220582	-0.525821	0.595576	-0.492288
Soil temperature	0.254875	0.160898	1	0.181325	-0.0818433	0.561697	-0.750725
CO ₂	-0.144756	-0.220582	0.181325	1	0.318603	-0.23215	0.0100295
Air pressure	-0.588404	-0.525821	-0.0818433	0.318603	1	0.0488437	0.197879
Air temperature	0.427518	0.595576	0.561697	-0.23215	0.0488437	1	-0.492288
Water volume	-0.724829	-0.492288	-0.750725	0.0100295	0.197879	-0.492288	1

Table 6

Pearson's correlations value ρ of sensor's parameters tomato's line I_{60} .

Property	Electrical conductivity	Soil humidity	Soil temperature	CO ₂	Air pressure	Air temperature	Water volume
Electrical conductivity	1	0.843224	0.699109	0.268819	-0.052491	0.218439	-0.893728
Soil humidity	0.843224	1	0.732316	0.162941	-0.103049	0.312731	-0.764701
Soil temperature	0.699109	0.732316	1	0.214677	0.000255456	0.644653	-0.717294
CO ₂	0.268819	0.162941	0.214677	1	0.318603	-0.23215	0.00513183
Air pressure	-0.052491	-0.103049	0.000255456	0.318603	1	0.0488437	0.200958
Air temperature	0.218439	0.312731	0.644653	-0.23215	0.0488437	1	-0.485407
Water volume	-0.893728	-0.764701	-0.717294	0.00513183	0.200958	-0.485407	1

Table 7

Pearson's correlations value ρ of sensor's parameters tomato's line I_{30} .

Property	Electrical conductivity	Soil humidity	Soil temperature	CO ₂	Air pressure	Air temperature	Water volume
Electrical conductivity	1	0.951482	0.432752	0.275139	-0.0934875	0.0639758	-0.854571
Soil humidity	0.951482	1	0.411506	0.32188	0.0161318	0.0574642	-0.798985
Soil temperature	0.432752	0.411506	1	0.151971	-0.0669304	0.743987	-0.604234
CO ₂	0.275139	0.32188	0.151971	1	0.318603	-0.23215	-0.0207285
Air pressure	-0.0934875	0.0161318	-0.0669304	0.318603	1	0.0488437	0.188897
Air temperature	0.0639758	0.0574642	0.743987	-0.23215	0.0488437	1	-0.465786
Water volume	-0.854571	-0.798985	-0.604234	-0.0207285	0.188897	-0.465786	1

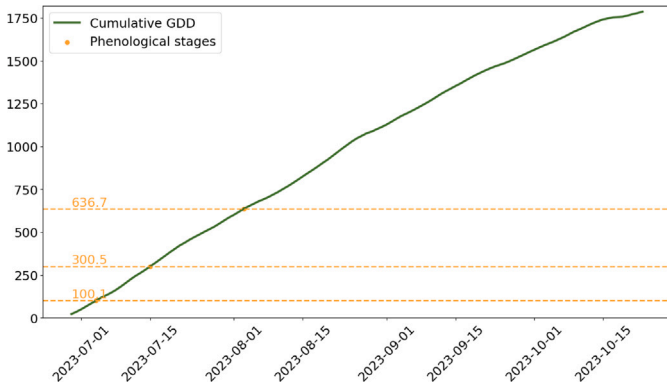


Fig. 8. Tomato's plant GDD accumulation values during summer 2023 and in particular during phenological stages (fruit set July 04, full flowering July 15 and fruit breaking August 03).

value can be calculated as defined by Saadi et al. (2015), and shown in Eq. (1):

$$GDD = \begin{cases} (T_{avg} - T_{base}) & \text{if } T_{avg} > T_{base} \text{ and } T_{avg} < T_{cutoff} \\ (T_{cutoff} - T_{base}) & \text{if } T_{avg} \geq T_{cutoff} \\ 0 & \text{if } T_{avg} \leq T_{base} \end{cases} \quad (1)$$

The accumulation of GDD values for the tomato's plants, calculated through a specific Processing Unit (using $T_{base} = 10\text{ }^\circ\text{C}$ and $T_{cutoff} = 32\text{ }^\circ\text{C}$) is shown in Fig. 8. In the same figure, GDD values during phenological stages, namely: fruit set (July 04, 2023), full flowering (July 15, 2023), and fruit breaking (August 03, 2023) are reported.

Another Processing Unit has been implemented to calculate the NHH curve. This indicator, specific to each crop, maps average temperatures to values between 0 and 1, helping to understand the impact of temperatures above or below the optimum growth temperatures. In particular, the optimal growth occurs within a specific air temperature range, delimited by the *Lower Cardinal* (LC) temperature (T_{base}) and the *Upper Cardinal* (UC) temperature (T_{cutoff}). Moreover, a sub-optimal range delimited by the *Lower Optimal* (LO) temperature and the *Upper Optimal* (UO) temperature has been defined. In this range, growth and development occur without thermal limitation, and the response of the NHH curve is set to 1. The values of the plant-related NHH curve have been calculated using the algorithm outlined by Ferrante and Mariani (2018), and defined as follows:

$$NHH = \begin{cases} 0 & \text{if } T \leq LC \text{ or } T \geq UC \\ 1 & \text{if } T \geq LO \text{ and } T \leq UO \\ m \cdot T + q & \text{if } T \geq LC \text{ and } T \leq LO \text{ where:} \\ & m = \frac{1}{(LO - LC)} \text{ and } q = 1 - \frac{LO}{(LO - LC)} \\ m \cdot T + q & \text{if } T \geq UO \text{ and } T < UC \text{ where:} \\ & m = -\frac{1}{(UC - UO)} \text{ and } q = 1 + \frac{UO}{(UC - UO)} \end{cases} \quad (2)$$

where: T represents the *average temperature*, $T_{base} = 10\text{ }^\circ\text{C}$, $T_{cutoff} = 32\text{ }^\circ\text{C}$, $LO = 22\text{ }^\circ\text{C}$, $LO = 22\text{ }^\circ\text{C}$, $UO = 26\text{ }^\circ\text{C}$. The obtained NHH curve is then shown in Fig. 9.

Finally, another Processing Unit has been developed to evaluate the Heat Units. In detail, these daily values are valuable tools for predicting harvest dates and determining the timing of successive plantings. As described in Perry et al. (1997), fruit production can be affected by several factors, including the interaction of light interception, ambient temperature and water consumption, with air temperature as the most important environmental factor. Heat Units are considered cumulative over time and are calculated daily using six different methods, as

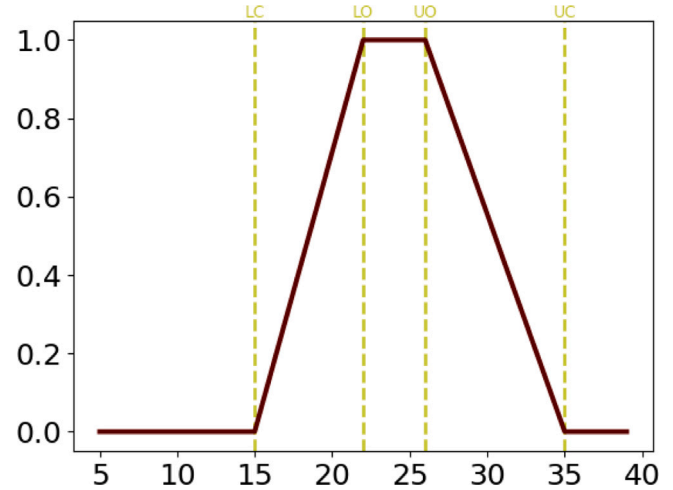


Fig. 9. NHH curve for tomato cultivation calculated through the Agriware Processing Unit.

defined by Machado et al. (2004) and listed below, and whose relevant variables include the following four parameters: (i) the daily maximum air temperature, denoted as T_x ; (ii) the daily minimum air temperature, denoted as T_n ; (iii) the *vegetation zero point* temperature, denoted as T_{base} and set at $10\text{ }^\circ\text{C}$ for the tomato's plant; (iv) the *cutoff* temperature, denoted as T_{cutoff} and set at $32\text{ }^\circ\text{C}$ for the tomato's plant.

1. Standard Day-Degrees: $[(T_x + T_n)/2] - T_{base}$;
2. Daily mean temperature: $(T_x + T_n)/2$;
3. Daily maximum temperature above T_{base} : $T_x - T_{base}$;
4. Daily maximum temperature: T_x ;
5. Daily maximum temperature above T_{base} with reduction of T_{cutoff} for plant development when T_x is higher then T_{cutoff} :
if $T_x \leq T_{cutoff}$: $T_x - T_{base}$
else if $T_x > T_{cutoff}$: $T_{cutoff} - (T_x - T_{cutoff}) - T_{base}$
6. Ontario Units: $(T_a + T_b)/2$ where:
 $T_a = 3.33 \cdot (T_x - 10) - 0.084 \cdot (T_x - 10)^2$
 $T_b = 1.8 \cdot (T_n - 4.4)$.

The accumulation over time of the six different calculated Heat Units is shown in Fig. 10.

Moreover, all the values described in Section 3.3 has been evaluated in correspondence to the data collected through IoT devices. For the sake of completeness, Tables 8–10 report the Pearson correlation's value ρ for tomato's lines I_{100} , I_{60} , and I_{30} , respectively.

The experimental data collected through the proposed IoT-based platform highlight that the irrigation line I_{60} achieves good results. Hence, irrigating this crop with only 60% of the water demand suggested by the Irriframe framework seems to be sufficient.

4. Discussion

In this work, the effects of different regimes of irrigation on tomato growth, yield and physiological traits have been studied. Given that it is well acknowledged that tomato is moderately sensitive to water stress that causes a reduction in fruit yield (as reported in Topçu et al., 2007; Jensen et al., 2010; Kuscu et al., 2014; Djurović et al., 2016), it can be argued that our experimental results for total yield are in agreement with the literature, as we obtained the highest results (in terms of total and marketable yields and fruit weight) under full irrigation conditions. However, it is worth noting that no significant differences have been

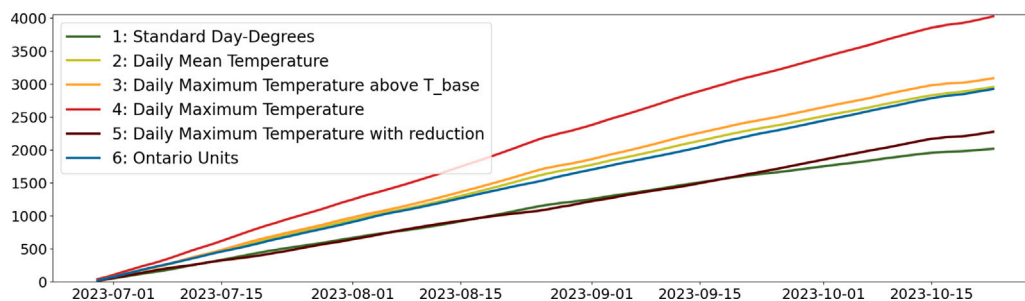


Fig. 10. Heat Units accumulation during time for tomato's crop.

Table 8

Pearson's correlations value ρ of sensor's parameters tomato's I_{100} and agronomic values.

	Electrical conductivity	Soil humidity	Soil temperature	CO ₂	Air pressure	Air temperature	Water volume
SPAD	0,670679261	0,813621423	0,998869404	-0,001185227	-0,319908644	-0,632386085	-0,946432843
a*	-0,205476043	0,94872077	0,548998536	0,808082129	0,578135064	0,254610319	-0,295452632
b*	0,875585002	-0,379697125	0,274942425	-0,973714676	-0,995523114	-0,898850768	-0,530988046
PI	0,697467644	0,79172071	0,999941432	-0,037909597	-0,354488062	-0,660408775	-0,957652973
RC/ABS	0,729686724	0,762788577	0,99938114	-0,083826263	-0,397116262	-0,694244059	-0,96988131
(1 - Vj)/Vj	0,705442669	0,784835569	0,999999933	-0,049088838	-0,364928876	-0,668769814	-0,9608148
Chlorophyll a	0,994704639	0,011724959	0,628578334	-0,80744844	-0,95338506	-0,99862418	-0,819741913
Chlorophyll b	-0,999433529	-0,14779927	-0,72864499	0,719579505	0,903404651	0,996461022	0,890106026
Chlorophyll tot	-0,260093192	-0,989003474	-0,868036771	-0,453617418	-0,14585028	0,21102563	0,696133866

Table 9

Pearson's correlations value ρ of sensor's parameters tomato's I_{60} and agronomic values.

	Electrical conductivity	Soil humidity	Soil temperature	CO ₂	Air pressure	Air temperature	Water volume
SPAD	0,605647734	0,648335366	0,468712731	-0,555275499	-0,791428244	-0,955732272	-0,964970246
a*	0,049829381	-0,004966316	0,21099884	0,960591893	0,999085274	0,920369563	0,568680065
b*	0,676833506	0,716148973	0,548614265	-0,475754157	-0,731329372	-0,924325998	-0,98514269
PI	0,909400629	0,930822547	0,829992394	-0,097279013	-0,409477191	-0,703902919	-0,974616495
RC/ABS	0,881701446	0,906226929	0,793603985	-0,159137986	-0,46555825	-0,746816267	-0,986678212
(1 - Vj)/Vj	0,882682775	0,907106055	0,794870234	-0,157080206	-0,463712871	-0,745428728	-0,986337037
Chlorophyll a	0,407514816	0,45693587	0,254165074	-0,730833853	-0,910292731	-0,997701838	-0,879343278
Chlorophyll b	0,760391081	0,79483245	0,645110884	-0,366606329	-0,644069746	-0,871769715	-0,99864149
Chlorophyll tot	0,553777317	0,598566321	0,411543683	-0,607079341	-0,828726208	-0,972520851	-0,946316741

Table 10

Pearson's correlations value ρ of sensor's parameters tomato's line I_{30} and agronomic values.

	Electrical conductivity	Soil humidity	Soil temperature	CO ₂	Air pressure	Air temperature	Water volume
SPAD	-0,688837094	-0,965768544	-0,192373662	-0,917478974	-0,996419097	-0,962603191	-0,652464521
a*	0,067112365	0,908834643	-0,478670965	0,451972166	0,712758234	0,91374952	0,986047371
b*	0,992970703	0,577869475	0,774455916	0,960173552	0,82100829	0,568086104	0,018556773
PI	0,333610831	-0,669241732	0,787310398	-0,061641766	-0,376604979	-0,678063833	-0,971325949
RC/ABS	0,197270145	-0,767381	0,692447382	-0,20184327	-0,503536662	-0,774980277	-0,995153593
(1 - Vj)/Vj	0,348884662	-0,65707983	0,797224736	-0,045415777	-0,361502841	-0,666031434	-0,967334546
Chlorophyll a	-0,42848578	-0,99850646	0,123173363	-0,747724402	-0,920389787	-0,999087485	-0,856215674
Chlorophyll b	0,046890611	-0,855445929	0,575496415	-0,347500644	-0,628289141	-0,861567098	-0,998586657
Chlorophyll tot	-0,309089059	-0,983258073	0,249407311	-0,656407764	-0,862654701	-0,985363172	-0,915392006

found between lines I_{60} and I_{100} for the marketable yield and the average weight of 100 tomatoes. Instead, comparable results in a semi-arid Mediterranean environment were already reported by Patanè et al. (2011), who tested 50% and 100% of the crop evapotranspiration (ET_c) irrigation restorations and found differences in the total yield but not in the marketable one. Besides, the adoption of a 60% irrigation regime resulted in a 11.12 m³ water saving across the season without affecting the ratio of marketable yield, compared to the full irrigation one. In contrast, the marketable ratio for I_{30} was greatly lowered by BER, a physiological disorder caused by calcium deficiency induced by soil water deficit, as detailed in Millones-Chanamé et al. (2019). Under water shortage conditions, IWUE and WUE are highly relevant indicators that reflect the effective use of water and help in its management whether the goal of the producers is to increase yields or profits (as indicated by Payero et al., 2008; Mukherjee et al., 2010). In this research, TYIWUE and MYIWUE values for the three water regimes

were similarly contrasting with several studies where IWUE increased due to water deficit (as detailed in Topçu et al., 2007; Kuscü et al., 2014; Patanè et al., 2020, 2021). A reasonable explanation for these results may be that, even though plants were properly watered up to 30 Days After Transplanting (DAT) to allow the crop establishment, the application of stress conditions began in the phenological stage of "tomato early blooms". Since flowering is one of the most sensitive phenological stages (as indicated by Nangare et al., 2016; Khapte et al., 2019), it is likely that watering tomato plants under full irrigation conditions for such a long time could have avoided flower abortion and, thus, enhanced IWUE.

Then, physiological disorders in stressed plants began with the onset of the trial and became more relevant over time, as reported in Tables 4 and 12. In agreement with Nemeskéri et al. (2015), SPAD was a good stress marker all along the experiment and its initial increase under severe dry conditions was already reported by Nemeskéri et al. (2019)

tomato plants. In fact, according to the obtained experimental results, the I_{60} irrigation regime demonstrated the best performances. This finding has positive environmental implications, as the I_{60} watering regime allowed farmers to save up to 823.70 m³/ha.

An interesting future research activity involves the extension of the functionalities and experimentation of the proposed IoT-based platform, including: (i) integrating new IoT Data Sources to expand the range of managed crops; (ii) implementing new AI-based Processing Units to predict the optimal harvesting time for tomato plants; and (iii) connecting the IoT-based platform to the digital model described in Preite et al. (2023a) in order to obtain a DT of the irrigation network for an improved distribution of the water across the field based on the actual demands of the different field sections and to allow a real-time faults' detection.

CRedit authorship contribution statement

Martina Galaverni: Conceptualization, Methodology, Validation, Formal analysis, Investigation, Resources, Data curation, Writing – original draft, Writing – review & editing, Visualization. **Giulia Oddi:** Conceptualization, Methodology, Validation, Formal analysis, Investigation, Resources, Data curation, Writing – original draft, Writing – review & editing, Visualization. **Luca Preite:** Conceptualization, Methodology, Validation, Formal analysis, Investigation, Resources, Data curation, Writing – original draft, Writing – review & editing, Visualization. **Laura Belli:** Conceptualization, Methodology, Validation, Formal analysis, Investigation, Resources, Data curation, Writing – original draft, Writing – review & editing, Visualization. **Luca Davoli:** Conceptualization, Methodology, Validation, Formal analysis, Investigation, Resources, Data curation, Writing – original draft, Writing – review & editing, Visualization. **Ilaria Marchioni:** Conceptualization, Methodology, Validation, Formal analysis, Investigation, Resources, Data curation, Writing – original draft, Writing – review & editing, Visualization. **Margherita Rodolfi:** Conceptualization, Methodology, Validation, Formal analysis, Investigation, Resources, Data curation, Writing – original draft, Writing – review & editing, Visualization. **Federico Solari:** Conceptualization, Methodology, Validation, Formal analysis, Investigation, Resources, Data curation, Writing – original draft, Writing – review & editing, Visualization. **Deborah Beghè:** Conceptualization, Methodology, Validation, Formal analysis, Investigation, Resources, Data curation, Writing – original draft, Writing – review & editing, Visualization. **Tommaso Ganino:** Conceptualization, Methodology, Validation, Formal analysis, Investigation, Resources, Data curation, Writing – original draft, Writing – review & editing, Visualization, Supervision, Project administration, Funding acquisition. **Giuseppe Vignali:** Conceptualization, Methodology, Validation, Formal analysis, Investigation, Resources, Data curation, Writing – original draft, Writing – review & editing, Visualization, Supervision, Project administration, Funding acquisition. **Gianluigi Ferrari:** Conceptualization, Methodology, Validation, Formal analysis, Investigation, Resources, Data curation, Writing – original draft, Writing – review & editing, Visualization, Supervision, Project administration, Funding acquisition.

Funding

This work has been supported by the Agritech project - “National Research Centre for Agricultural Technologies,” project code CN00000022, funded under the National Recovery and Resilience Plan (NRRP), Mission 4 Component 2 Investment 1.4 - Call for tender no. 3138 of 16/12/2021 of Italian Ministry of University and Research funded by the European Union – NextGenerationEU, Concession Decree no. 1032 of 17/06/2022 adopted by the Italian Ministry of University and Research (MUR). This work has been also supported by the SMALLDERS research project - “Smart Models for Agrifood Local value chain based on Digital technologies for Enabling covid-19 Resilience and

Table 11

Branch length and percentage composition of tomato plant biomass on total dry weight.

Water regime	Branch length (cm)	Epigeal biomass (%)	Hypogeal biomass (%)
I_{30}	105.47 ± 2.22 ^c	83.53 ± 3.13	16.47 ± 3.13
I_{60}	123.07 ± 0.57 ^b	79.80 ± 1.27	20.20 ± 1.27
I_{100}	134.27 ± 2.62 ^a	76.57 ± 4.60	23.43 ± 4.60

Data are reported in mean ± standard error. Different letters indicate significant differences at $p < 0.05$ by Tukey's test.

Table 12

Effects of the irrigation treatments on SPAD index and Lab* space parameters.

Time	Water regime	SPAD	L*	a*	b*
S_1	I_{30}	57.55 ± 0.49	38.51 ± 0.28	-11.97 ± 0.16	14.65 ± 0.29
	I_{60}	55.68 ± 0.57	39.61 ± 0.25	-11.52 ± 0.18	16.48 ± 0.35
	I_{100}	53.61 ± 0.76	40.13 ± 0.23	-10.66 ± 0.20	17.55 ± 0.39
S_2	I_{30}	59.32 ± 0.73	38.51 ± 0.35	-10.00 ± 0.18	12.53 ± 0.29
	I_{60}	53.31 ± 0.75	38.09 ± 0.37	-12.15 ± 0.21	15.58 ± 0.42
	I_{100}	49.84 ± 0.95	38.26 ± 0.33	-13.43 ± 0.25	17.65 ± 0.56
S_3	I_{30}	45.81 ± 1.67	42.07 ± 0.47	-8.92 ± 0.24	14.25 ± 0.54
	I_{360}	50.58 ± 0.93	40.91 ± 0.42	-10.37 ± 0.29	14.93 ± 0.58
	I_{100}	49.14 ± 0.77	39.14 ± 0.39	-11.91 ± 0.27	16.00 ± 0.43

The data are reported in mean ± standard error.

Table 13

Two-way ANOVAs regarding physiological measurements on tomato leaves.

Variable	Effect of time	Effect of treatment	Effect of interaction
SPAD	<0.001***	<0.001***	<0.001***
Chl a	<0.001***	0.0142*	0.040*
Chl b	NS	NS	0.020*
Chl tot	0.001**	0.030*	0.029*
Carotenoids	<0.001***	0.001**	NS
L*	<0.001***	NS	<0.001***
a*	<0.001***	<0.001***	<0.001***
b*	0.001**	<0.001***	0.015*
PIABS	<0.001***	NS	0.043*
RC/ABS	<0.001***	NS	0.043*
Area	<0.001***	0.025*	0.019*
(1-Vj)/Vj	0.001**	NS	NS

NS = not significant at $\alpha = 0.05$.

* Stars represent different p -value thresholds: < 0.001 .

** Stars represent different p -value thresholds: < 0.01 .

*** Stars represent different p -value thresholds: < 0.05 .

Sustainability,” co-funded by the PRIMA Program - Section 2 Call multi-topics 2021, through the following National Authorities: MUR, Italy; State Research Agency (AEI, Spain); Agence Nationale de la Recherche (ANR, France); Ministry of Higher Education and Scientific Research (Tunisia). The work reflects only the authors' views and opinions; neither the European Union nor the European Commission can be considered responsible for any use that may be made of the information it contains.

Declaration of competing interest

The authors declare that they have no known competing financial interests or personal relationships that could have appeared to influence the work reported in this paper.

Appendix. Supplementary materials

This section contains supplementary material that expands on the data and analyses discussed in the main text. These include additional figures and tables that provide further insight (see Tables 11–13).

Data availability

Data are available at the following public repository: [Belli et al. \(2024\)](#).

References

- Alharbi, H.A., Aldossary, M., 2021. Energy-efficient edge-fog-cloud architecture for IoT-based smart agriculture environment. *IEEE Access* 9, 110480–110492. <http://dx.doi.org/10.1109/ACCESS.2021.3101397>.
- ANBI, 2024. Home page. <https://www.anbi.it/?lang=en>. (Accessed 26 June 2024).
- Antunović Dunić, J., et al., 2023. Comparative analysis of primary photosynthetic reactions assessed by OJIP kinetics in three brassica crops after drought and recovery. *Appl. Sci.* 13 (5), 3078. <http://dx.doi.org/10.3390/app13053078>.
- Azienda Agraria Sperimentale Stuard, 2024. Home page. <https://www.stuard.it/>. (Accessed 26 June 2024).
- Bartlett, M.S., 1937. Properties of sufficiency and statistical tests. *Proc. R. Soc. Lond. Ser. A Math. Phys. Eng. Sci.* 160 (901), 268–282. <http://dx.doi.org/10.1098/rspa.1937.0109>, URL: <http://www.jstor.org/stable/96803>. (Accessed 04 October 2024).
- Battilani, A., Ventura, F., 1997. Influence of water table, irrigation and rootstock on transpiration rate and fruit growth of peach trees. In: *ISHS Acta Horticulturae 449: II International Symposium on Irrigation of Horticultural Crops*. <http://dx.doi.org/10.17660/ActaHortic.1997.449.72>.
- Belli, L., Davoli, L., Ferrari, G., 2023. Smart city as an urban intelligent digital system: The case of parma. *Computer* 56 (7), 106–109. <http://dx.doi.org/10.1109/MC.2023.3267245>.
- Belli, L., Davoli, L., Oddi, G., Preite, L., Galaverni, M., Ganino, T., Ferrari, G., 2024. IoT-based data collection in a tomato cultivation under different irrigation regimes. <http://dx.doi.org/10.17632/35wh56287y>, URL: <https://data.mendeley.com/datasets/35wh56287y>.
- Bleiholder, H., et al., 2001. Growth Stages of Mono-And Dicotyledonous Plants. In: *BBCB Monograph*, vol. 158, Federal Biological Research Centre for Agriculture and Forestry, Berlin/Braunschweig, Germany, <http://dx.doi.org/10.5073/20180906-074619>.
- Boyaci, S., et al., 2024. Evaluation of crop water stress index (CWSI) for high tunnel greenhouse tomatoes under different irrigation levels. *Atmosphere* 15 (2), 205. <http://dx.doi.org/10.3390/atmos15020205>.
- Chambers, J.M., Freeny, A.E., Heiberger, R.M., 1992. Analysis of variance; designed experiments. *Statist. Models* 5 145–194.
- Connectivity Standard Alliance, 2024. ZigBee. <https://csa-iot.org/all-solutions/zigbee/>. (Accessed 03 October 2024).
- Conover, W.J., Johnson, M.E., Johnson, M.M., 1981. A comparative study of tests for homogeneity of variances, with applications to the outer continental shelf bidding data. *Technometrics* 23 (4), 351–361. <http://dx.doi.org/10.1080/00401706.1981.10487680>.
- Cramer, W., et al., 2018. Climate change and interconnected risks to sustainable development in the Mediterranean. *Nature Clim. Change* 8 (11), 972–980. <http://dx.doi.org/10.1038/s41558-018-0299-2>.
- Dagar, R., Som, S., Khatri, S.K., 2018. Smart farming—IoT in agriculture. In: 2018 International Conference on Inventive Research in Computing Applications. *ICIRCA*, IEEE, pp. 1052–1056. http://dx.doi.org/10.1007/978-3-030-58675-1_114-1.
- Davoli, L., et al., 2024. Coap-based digital twin modelling of heterogeneous IoT scenarios. In: *Proceedings of the 10th International Food Operations and Processing Simulation Workshop*. *FoodOPS 2024*, La Laguna, Spain, pp. 1–5. <http://dx.doi.org/10.46354/i3m.2024.foodops.016>, 16.
- de Carvalho Silva, J., Rodrigues, J.J., Alberti, A.M., Solic, P., Aquino, A.L., 2017. LoRaWAN—A low power WAN protocol for internet of things: A review and opportunities. In: 2017 2nd International Multidisciplinary Conference on Computer and Energy Science. *SpliTech*, IEEE, pp. 1–6.
- Derscheid, L.A., Lytle, W.F., 1981. Growing degree days (GDD). *SDSU Ext. Fact Sheets*.
- Djurović, N., et al., 2016. Effect of irrigation regime and application of kaolin on yield, quality and water use efficiency of tomato. *Sci. Horticul.* 201, 271–278. <http://dx.doi.org/10.1016/j.scienta.2016.02.017>.
- Dong, Y., et al., 2024. Implementation of an in-field IoT system for precision irrigation management. *Front. Water* 6, 1353597. <http://dx.doi.org/10.3389/frwa.2024.1353597>.
- FAO, 2023. Agricultural production statistics 2000–2022. *FAO*, <http://dx.doi.org/10.4060/cc9205en>.
- Ferrante, A., Mariani, L., 2018. Agronomic management for enhancing plant tolerance to abiotic stresses: High and low values of temperature, light intensity, and relative humidity. *Horticultrae* 4 (3), 21. <http://dx.doi.org/10.3390/horticultrae4030021>.
- Flawnex, 2024. Home page. <https://flawnex.com/>. (Accessed 26 June 2024).
- Gerszberg, A., Hnatuszko-Konka, K., 2017. Tomato tolerance to abiotic stress: a review of most often engineered target sequences. *Plant Growth Regul.* 83, 175–198. <http://dx.doi.org/10.1007/s10725-017-0251-x>.
- Giuliani, M.M., et al., 2016. Water saving strategies assessment on processing tomato cultivated in Mediterranean region. *Ital. J. Agron.* 11 (1), 69–76. <http://dx.doi.org/10.4081/ija.2016.738>.
- Giuliani, M.M., et al., 2017. Deficit irrigation and partial root-zone drying techniques in processing tomato cultivated under Mediterranean climate conditions. *Sustainability* 9 (12), 2197. <http://dx.doi.org/10.3390/su9122197>.
- Graves, S., et al., 2023. multcompView: Visualizations of paired comparisons. *R Package Version 0.1-8*.
- Gutiérrez, J., et al., 2014. Automated irrigation system using a wireless sensor network and GPRS module. *IEEE Trans. Instrum. Meas.* 63 (1), 166–176. <http://dx.doi.org/10.1109/TIM.2013.2276487>.
- Hammami, Z., et al., 2024. The efficiency of chlorophyll fluorescence as a selection criterion for salinity and climate aridity tolerance in barley genotypes. *Front. Plant Sci.* 15, 1324388. <http://dx.doi.org/10.3389/fpls.2024.1324388>.
- Hnatiuc, M., Paun, M., Kapsamun, D., 2022. IoT sensors system for vineyard monitoring. In: 2022 7th International Conference on Information and Network Technologies. *ICINT*, IEEE, pp. 46–51. <http://dx.doi.org/10.1109/ICINT55083.2022.00015>.
- International Commission on Illumination (CIE), Technical Committee ISO/TC 274, 2019. *Colorimetry – Part 4: CIE 1976 L*a*b* Colour Space. Standard 2019*, International Organization for Standardization, Geneva, CH.
- Irriframe, 2024. Home page. <https://www.irriframe.it/Irriframe>. (Accessed 26 June 2024).
- Jani, K.A., Chaubey, N.K., 2022. A novel model for optimization of resource utilization in smart agriculture system using IoT (SMAIoT). *IEEE Internet Things J.* 9 (13), 11275–11282. <http://dx.doi.org/10.1109/JIOT.2021.3128161>.
- Jedemski, C., et al., 2015. Impact of drought, heat, and their combination on chlorophyll fluorescence and yield of wild barley (*Hordeum spontaneum*). *J. Bot.* 2015 (1), 120868. <http://dx.doi.org/10.1155/2015/120868>.
- Jensen, M., 1968. Water consumption by agricultural plants. In: *Water Deficits and Plant Growth*. vol. 2, Academic Press, New York, pp. 1–22. <http://dx.doi.org/10.1093/jxb/er1165>.
- Jensen, C.R., et al., 2010. Deficit irrigation based on drought tolerance and root signalling in potatoes and tomatoes. *Agric. Water. Manag.* 98 (3), 403–413. <http://dx.doi.org/10.1016/j.agwat.2010.10.018>.
- Kanthavel, D., et al., 2022. Energy efficient resource allocation algorithm for agriculture IoT. *Wirel. Pers. Commun.* 125, 1–23. <http://dx.doi.org/10.1007/s11277-022-09607-z>.
- Kassambara, A., 2023a. Ggcorrplot: Visualization of a correlation matrix using ‘Ggplot2’. *R package version 0.1.3* (2019).
- Kassambara, A., 2023b. ggpubr: ‘ggplot2’ based publication ready plots. p. 2, *R package version*.
- Kassambara, A., et al., 2020. Pipe-friendly framework for basic statistical tests. *R package version 0.6.0*.
- Khapte, P., et al., 2019. Deficit irrigation in tomato: Agronomical and physio-biochemical implications. *Sci. Horticul.* 248, 256–264. <http://dx.doi.org/10.1016/j.scienta.2019.01.006>.
- Kim, S., Lee, M., Shin, C., 2018. IoT-based strawberry disease prediction system for smart farming. *Sensors* 18 (11), 4051. <http://dx.doi.org/10.3390/s18114051>.
- Kuscu, H., et al., 2014. Optimizing levels of water and nitrogen applied through drip irrigation for yield, quality, and water productivity of processing tomato (*Lycopersicon esculentum* Mill.). *Horticul. Environ. Biotechnol.* 55, 103–114. <http://dx.doi.org/10.1007/s13580-014-0180-9>.
- Lakshmi, G.P., et al., 2023. An intelligent IoT sensor coupled precision irrigation model for agriculture. *Measurement* 25, 100608. <http://dx.doi.org/10.1016/j.measen.2022.100608>.
- LoRa Alliance, 2024. LoRaWAN specification v1.1. <https://resources.lora-alliance.org/technical-specifications/lorawan-specification-v1-1>. (Accessed 26 June 2024).
- Machado, R., et al., 2004. Prediction of optimal harvest date for processing tomato based on the accumulation of daily heat units over the fruit ripening period. *J. Horticul. Sci. Biotechnol.* 79 (3), 452–457. <http://dx.doi.org/10.1080/14620316.2004.11511789>.
- Marcheriz, I., Fitriani, E., 2023. Design of IoT-based tomato plant growth monitoring system in the yard. *Sinkron* 8, 762–770. <http://dx.doi.org/10.33395/sinkron.v8i2.12226>.
- Mclimate T-valve, 2024. Mclimate LoRaWAN T-valve. <https://mclimate.eu/products/mclimate-t-valve>. (Accessed 26 June 2024).
- McMaster, G.S., Wilhelm, W., 1997. Growing degree-days: one equation, two interpretations. *Agric. Forest Meteorol.* 87 (4), 291–300.
- Medyouni, I., et al., 2021. Effects of water deficit on leaves and fruit quality during the development period in tomato plant. *Food Sci. Nutr.* 9 (4), 1949–1960. <http://dx.doi.org/10.1002/fsn3.2160>.
- Mendiburu, F., 2010. *Agricolae: Statistical procedures for agricultural research*. pp. 1–8, *R package version 1*.
- Miles, B., et al., 2020. A study of LoRaWAN protocol performance for IoT applications in smart agriculture. *Comput. Commun.* 164, 148–157. <http://dx.doi.org/10.1016/j.comcom.2020.10.009>.
- Milesight EM500-CO2, 2024. Milesight EM500-SMTC environmental sensor. <https://www.milesight.com/iot/product/lorawan-sensor/em500-co2>. (Accessed 26 June 2024).

- Milesight EM500-SMTC, 2024. Milesight EM500-SMTC soil sensor. <https://www.milesight.com/iot/product/lorawan-sensor/em500-smtc>. (Accessed 26 June 2024).
- Milesight UG67, 2024. UG67 outdoor LoRaWAN gateway. <https://www.milesight.com/iot/product/lorawan-gateway/ug67>. (Accessed 26 June 2024).
- Millones-Chanamé, C.E., et al., 2019. Inheritance of blossom end rot resistance induced by drought stress and of associated stomatal densities in tomatoes. *Euphytica* 215, 1–10. <http://dx.doi.org/10.1007/s10681-019-2444-z>.
- MQTT, 2024. MQTT protocol: The standard for IoT messaging. <https://mqtt.orghttps://mqtt.org>. (Accessed 26 June 2024).
- Mukherjee, A., Kundu, M., Sarkar, S., 2010. Role of irrigation and mulch on yield, evapotranspiration rate and water use pattern of tomato (*Lycopersicon esculentum* L.). *Agricult. Water. Manag.* 98 (1), 182–189. <http://dx.doi.org/10.1016/j.agwat.2010.08.018>.
- Nanda, A., et al., 2021. Multiple comparison test by tukey's honestly significant difference (HSD): Do the confident level control type I error. *Int. J. Stat. Appl. Math.* 6 (1), 59–65. <http://dx.doi.org/10.22271/math.2021.v6.i1a.636>.
- Nangare, D., et al., 2016. Growth, fruit yield and quality of tomato (*Lycopersicon esculentum* Mill.) as affected by deficit irrigation regulated on phenological basis. *Agricult. Water. Manag.* 171, 73–79. <http://dx.doi.org/10.1016/j.agwat.2016.03.016>.
- Nemeskéri, E., et al., 2015. Relationships between stomatal behaviour, spectral traits and water use and productivity of green peas (*Pisum sativum* L.) in dry seasons. *Acta Physiol. Plant.* 37, 1–16. <http://dx.doi.org/10.1007/s11738-015-1776-0>.
- Nemeskéri, E., et al., 2019. Physiological factors and their relationship with the productivity of processing tomato under different water supplies. *Water* 11 (3), 586. <http://dx.doi.org/10.3390/w11030586>.
- Obaideen, K., et al., 2022. An overview of smart irrigation systems using IoT. *Energy Nexus* 7, 100124. <http://dx.doi.org/10.1016/j.nexus.2022.100124>.
- Oddi, G., et al., 2024. Optimizing tomato production through IoT-based smart data collection and analysis. In: 2024 IEEE 20th International Conference on Automation Science and Engineering. CASE, Bari, Italy, pp. 45–50. <http://dx.doi.org/10.1109/CASE59546.2024.10711738>.
- Palconit, M.G.B., et al., 2020. IoT-based precision irrigation system for eggplant and tomato. In: 9th Int. Symp. Comput. Intell. Ind. Appl. pp. 0–6, November.
- Patanè, C., Tringali, S., Sortino, O., 2011. Effects of deficit irrigation on biomass, yield, water productivity and fruit quality of processing tomato under semi-arid Mediterranean climate conditions. *Sci. Horticult.* 129 (4), 590–596. <http://dx.doi.org/10.1016/j.scienta.2011.04.030>.
- Patanè, C., et al., 2020. Physiological and agronomic responses of processing tomatoes to deficit irrigation at critical stages in a semi-arid environment. *Agronomy* 10 (6), 800. <http://dx.doi.org/10.3390/agronomy10060800>.
- Patanè, C., et al., 2021. Fruit yield, polyphenols, and carotenoids in long shelf-life tomatoes in response to drought stress and rewatering. *Agronomy* 11 (10), 1943. <http://dx.doi.org/10.3390/agronomy11101943>.
- Payero, J.O., et al., 2008. Effect of irrigation amounts applied with subsurface drip irrigation on corn evapotranspiration, yield, water use efficiency, and dry matter production in a semiarid climate. *Agricult. Water. Manag.* 95 (8), 895–908. <http://dx.doi.org/10.1016/j.agwat.2008.02.015>.
- Pereira, L., Allen, R., Smith, M., 2015. Crop evapotranspiration estimation with FAO56: Past and future. *Agricult. Water. Manag.* 147, 4–20. <http://dx.doi.org/10.1016/j.agwat.2014.07.031>.
- Perry, K.B., et al., 1997. Heat units to predict tomato harvest in the southeast USA. *Agricult. Forest. Meteorol.* 84 (3–4), 249–254. <http://dx.doi.org/10.1080/14620316.2004.11511789>.
- Popovic, T., et al., 2017. Architecting an IoT-enabled platform for precision agriculture and ecological monitoring: A case study. *Comput. Electron. Agric.* 2017, 255–265. <http://dx.doi.org/10.1016/j.compag.2017.06.008>.
- Preite, L., Solari, F., Vignali, G., 2023a. A digital model application to optimize water consumption in agriculture. In: Proceedings of the International Food Operations and Processing Simulation Workshop. FOODOPS, Vol. 2023-September, <http://dx.doi.org/10.46354/i3m.2023.foodops.006>.
- Preite, L., Solari, F., Vignali, G., 2023b. Technologies to optimize the water consumption in agriculture: A systematic review. *Sustainability* 15 (7), <http://dx.doi.org/10.3390/su15075975>.
- Preite, L., Vignali, G., 2024. Artificial intelligence to optimize water consumption in agriculture: A predictive algorithm-based irrigation management system. *Comput. Electron. Agric.* 223, 109126. <http://dx.doi.org/10.1016/j.compag.2024.109126>.
- Purcell, W., Neubauer, T., Mallinger, K., 2023. Digital twins in agriculture: challenges and opportunities for environmental sustainability. *Curr. Opin. Environ. Sustain.* 61, 101252. <http://dx.doi.org/10.1016/j.cosust.2022.101252>.
- R Core Team, 2024. The R project for statistical computing. <https://www.r-project.org>. (Accessed 26 June 2024).
- Rodolfi, M., et al., 2021. The effect of different organic foliar fertilization on physiological and chemical characters in hop (*Humulus lupulus* L., cv Cascade) leaves and cones. *Appl. Sci.* 11 (15), 6778. <http://dx.doi.org/10.3390/app11156778>.
- Rohith, M., Sainivedhana, R., Sabiyath Fatima, N., 2021. IoT enabled smart farming and irrigation system. In: 2021 5th International Conference on Intelligent Computing and Control Systems. ICICCS, pp. 434–439. <http://dx.doi.org/10.1109/ICICCS51141.2021.9432085>.
- Rolando, J.L., et al., 2015. Leaf greenness as a drought tolerance related trait in potato (*Solanum tuberosum* L.). *Environ. Exp. Bot.* 110, 27–35. <http://dx.doi.org/10.1016/j.envexpbot.2014.09.006>.
- Ross, A., Willson, V.L., 2017. One-way anova. In: Basic and Advanced Statistical Tests: Writing Results Sections and Creating Tables and Figures. SensePublishers, Rotterdam, pp. 21–24. http://dx.doi.org/10.1007/978-94-6351-086-8_5, (Chapter 5).
- Saadi, S., et al., 2015. Climate change and mediterranean agriculture: Impacts on winter wheat and tomato crop evapotranspiration, irrigation requirements and yield. *Agricult. Water. Manag.* 147, 103–115. <http://dx.doi.org/10.1016/j.agwat.2014.05.008>.
- Sadowski, S., Spachos, P., 2020. Wireless technologies for smart agricultural monitoring using internet of things devices with energy harvesting capabilities. *Comput. Electron. Agric.* 172, 105338. <http://dx.doi.org/10.48550/arXiv.2005.02477>.
- Seyar, M.H., Ahamed, T., 2023. Development of an IoT-based precision irrigation system for tomato production from indoor seedling germination to outdoor field production. *Appl. Sci.* 13 (9), 5556. <http://dx.doi.org/10.3390/app13095556>.
- Shapiro, S.S., Wilk, M.B., 1965. An analysis of variance test for normality (complete samples). *Biometrika* 52 (3–4), 591–611. <http://dx.doi.org/10.1093/biomet/52.3-4.591>.
- Sousaraei, N., et al., 2021. Screening of tomato landraces for drought tolerance based on growth and chlorophyll fluorescence analyses. *Horticult. Environ. Biotechnol.* 62, 521–535. <http://dx.doi.org/10.1007/s13580-020-00328-5>.
- Strasserf, R.J., Srivastava, A., Govindjee, 1995. Polyphasic chlorophyll a fluorescence transient in plants and cyanobacteria. *Photochem. Photobiol.* 61 (1), 32–42. <http://dx.doi.org/10.1111/j.1751-1097.1995.tb09240.x>.
- Talkpool OY1310, 2024. Talkpool OY1310 LoRaWAN water meter. <https://talkpool.com/shop/oy1310/>. (Accessed 26 June 2024).
- Tobiasz-Salach, R., et al., 2019. Can photosynthetic performance of oat (*avena sativa* L.) plants be used as bioindicator for their proper growth conditions. *Chiang Mai J. Sci.* 46 (5), 880–895.
- Topçu, S., et al., 2007. Yield response and N-fertiliser recovery of tomato grown under deficit irrigation. *Eur. J. Agron.* 26 (1), 64–70. <http://dx.doi.org/10.1016/j.eja.2006.08.004>.
- Trilles, S., et al., 2020. Development of an open sensorized platform in a smart agriculture context: A vineyard support system for monitoring mildew disease. *Sustain. Comput. Inform. Syst.* 28, 100309. <http://dx.doi.org/10.1016/j.suscom.2019.01.011>.
- TTN, 2024. The things network platform. <https://www.thethingsnetwork.org>. (Accessed 26 June 2024).
- Valcárcel, M., et al., 2020. Controlled deficit irrigation as a water-saving strategy for processing tomato. *Sci. Horticult.* 261, 108972. <http://dx.doi.org/10.1016/j.scienta.2019.108972>.
- Wei, T., et al., 2021. Package “corrplot”: Visualization of a correlation matrix. Version 0.84.
- Wickham, H., 2016. *ggplot2: Elegant Graphics for Data Analysis*. Springer-Verlag, New York.
- WiFi Alliance, 2024. WiFi alliance. <https://www.wi-fi.org>. (Accessed 03 October 2024).
- Zhang, H., et al., 2022. LoRaWAN based internet of things (IoT) system for precision irrigation in plasticulture fresh-market tomato. *Smart Agric. Technol.* 2, 100053. <http://dx.doi.org/10.1016/j.atech.2022.100053>.
- Zhou, R., et al., 2017. Drought stress had a predominant effect over heat stress on three tomato cultivars subjected to combined stress. *BMC Plant Biol.* 17, 1–13. <http://dx.doi.org/10.1186/s12870-017-0974-x>.